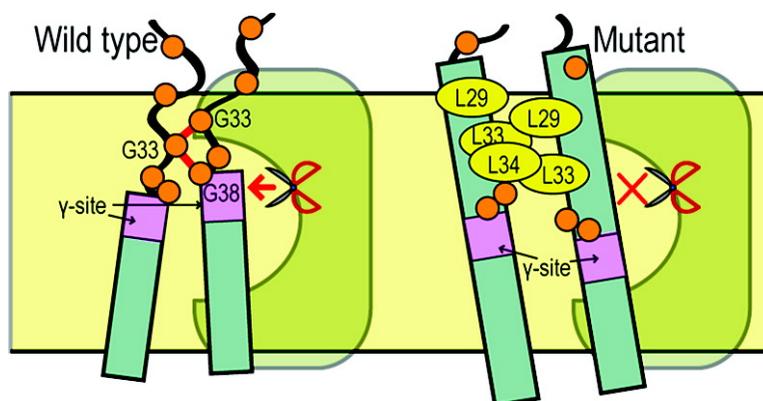## Communication

Transmembrane Structures of Amyloid Precursor Protein Dimer Predicted by Replica-Exchange Molecular Dynamics Simulations

Naoyuki Miyashita, John E. Straub, D. Thirumalai, and Yuji Sugita

More About This Article

Additional resources and features associated with this article are available within the HTML version:

- Supporting Information
- Access to high resolution figures
- Links to articles and content related to this article
- Copyright permission to reproduce figures and/or text from this article

View the Full Text HTML

Transmembrane Structures of Amyloid Precursor Protein Dimer Predicted by Replica-Exchange Molecular Dynamics Simulations

Naoyuki Miyashita,[†] John E. Straub,[‡] D. Thirumalai,[§] and Yuji Sugita*,[||]

RIKEN Computational Science Research Program, Molecular Scale Team, 2-1 Hirosawa, Wako, Saitama 351-0198, Japan, Department of Chemistry, Boston University, 590 Commonwealth Avenue Boston, Massachusetts 02215-2521, Department of Chemistry and Biochemistry and Biophysics Program, Institute for Physical Science and Technology, University of Maryland, College Park, Maryland 20742, and RIKEN Advanced Science Institute, 2-1 Hirosawa, Wako, Saitama 351-0198, Japan

Received November 25, 2008; E-mail: sugita@riken.jp

Aggregation of amyloid β peptide (Aβ) in the brain is the primary element in the pathogenesis of Alzheimer's disease (AD).[1] Aβ is produced from amyloid precursor protein (APP), which is a type-I transmembrane (TM) glycoprotein in neural and non-neural cells. APP is first cleaved on the β-site by β-secretase, and the extracellular domain of APP is dissociated from the remaining protein (APP-C99). γ-Secretase then cleaves the γ-site (Gly$_{38}$–Thr$_{43}$), which is located in the TM domain of APP-C99. Finally, Aβ is released to the extracellular region. Because the γ-site contains several cleavage points [see Supporting Figure (SF) 1 in the Supporting Information], Aβ's having different chain lengths are observed. Of these, Aβ_{1-40} and Aβ_{1-42} are primary and secondary isoforms, respectively.

Structural information on Aβ and its aggregated forms has been accumulated by NMR spectroscopy and X-ray crystallography.[2] A number of molecular dynamics (MD) simulations of the aggregation of Aβ in solution have also been performed.[3] In contrast, little is known about the TM structures of APP and APP-C99. Since the amyloid accumulation depends on the chain length of Aβ, it is relevant to understand how Aβ is cleaved by γ-secretase and released from APP-C99. To address this key question, we have determined the monomer structure of the APP-C99 fragment (Aβ_{1-55}), which has two α-helical regions from His$_{13}$ to Val$_{18}$ and from Ala$_{30}$ to Lys$_{53}$, by replica-exchange MD (REMD) simulations.[4]

APP-C99 contains three Gly-XXX-Gly motifs in the TM and juxtamembrane (JM) regions. This motif is known to promote dimerization of polypeptides via C$_\alpha$–H···O hydrogen bonds between two segments in a membrane environment. A pairwise replacement of Gly (Gly$_{29}$ and Gly$_{33}$) with Leu (Leu$_{29}$ and Leu$_{33}$) in APP enhances the homodimerization but leads to a drastic reduction of Aβ_{1-40} and Aβ_{1-42} secretion.[5] To resolve this apparent discrepancy, it would be useful to predict the homodimer conformations of APP-C99 in the membrane. Understanding these homodimer conformations is essential for elucidating the last step in the formation of Aβ-associated AD.

We performed REMD simulations of two APP fragments (Aβ_{23-55}) in a membrane environment for both the wild-type (WT) sequence and a mutant in which Gly$_{29}$ and Gly$_{33}$ are replaced by Leu$_{29}$ and Leu$_{33}$. MMTSB toolsets with the CHARMM 19 EEF1.1 force field were used for the calculations[6] (the simulation details are given in the Supporting Information). The effects of the solvent and the membrane on the APP fragments were included implicitly using the IMM1 implicit membrane model.[7]
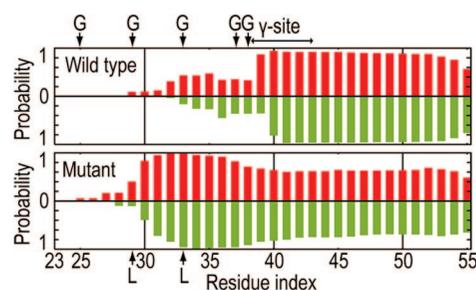

[†] RIKEN Computational Science Research Program.
[‡] Boston University.
[§] University of Maryland.
[||] RIKEN Advanced Science Institute.

Figure 1. α-Helical content of each residue in the (a) WT and (b) mutant proteins at 300 K. The α-helical residue was defined with DSSP.[8] Green and red lines represent the α-helical content for two fragments in the WT and the mutant. The locations of Gly, mutated Leu, and the γ-site are explicitly shown.
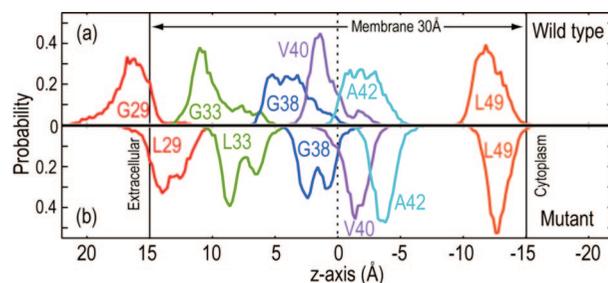

Figure 2. Distributions of the C$_\alpha$ positions of G29 and L29 (red), G33 and L33 (green), G38 (blue), V40 (purple), A42 (cyan), and L49 (orange) along the z axis for the (a) WT and (b) mutant proteins.

At 300 K, secondary and tertiary structures of the mutant APP fragments differ from those of the WT. In Figure 1, we compare the α-helicity of each residue in the WT with the corresponding one in the mutant. The similarity of α-helicity in the top (red) and bottom (green) plots indicates that the REMD simulations were able to sample all of the possible configurations of the APP fragments in the membrane. Marked contrasts in the α-helicities of the WT and the mutant are observed for residues 29–38. This region was observed to be unwound in the WT, whereas it formed an α-helix in the mutant. In Figure 2, Leu$_{29}$ in the mutant was located in the membrane, whereas Gly$_{29}$ in the WT was in the extracellular region. The position of Leu$_{49}$ was not altered by the mutation. Each mutant APP fragment was, therefore, more tilted (see SF 3). As a result, the γ-site in the mutant was shifted toward the center of the membrane.

We also investigated the homodimer conformations of the WT and mutant APP fragments at 300 K by principal component analysis (PCA)[9] of the backbone atoms in the region from Gly$_{29}$ to
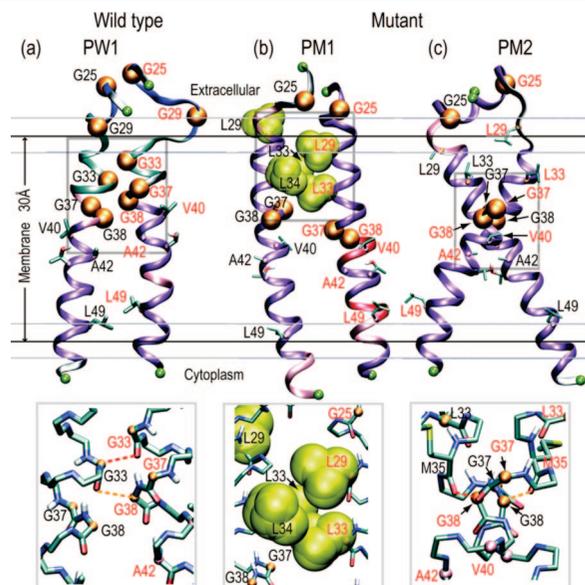
Figure 3. Structures of major dimer conformations of (a) the WT and (b, c) the mutant. Gray boxes indicate specific dimerization sites and are enlarged as insets at the bottom. Red and orange dashes indicate strong and medium $C_\alpha-H\cdots O$ hydrogen bonds, respectively.

Thr_{43}. By using the first and third principal components (PC1 and PC3), we obtained two major peaks for the mutant (PM1, 65.4%; PM2, 28.5%) and several other peaks for the WT (see SF 4). Because of the backbone flexibility observed in the WT, PCA could not classify major dimer structures. Instead, we used $C_\alpha-H\cdots O$ hydrogen bonds between the two fragments for these classifications, as shown in SF 5.

We observed three different types of homodimer conformation of APP fragments in the membrane. The first type, observed only in the WT, was stabilized by $C_\alpha-H\cdots O$ hydrogen bonds between the two APP fragments. These bonds are the most characteristic interaction between two fragments that contain Gly-XXX-Gly motifs. Because of the three Gly-XXX-Gly motifs in the WT APP fragments, multiple $C_\alpha-H\cdots O$ hydrogen bonds were observed. Of these, the hydrogen bonds involving Gly_{33} and Gly_{38} were essential for the dimerization of the WT APP fragments (Figure 3a inset and SF 6). This causes a partial unwinding of the α-helices in residues 29−38, as shown in Figure 1. Solid-state NMR spectroscopy has also shown that the glycines in the Gly-XXX-Gly motif lie at the dimer interface.[10]

In the second type of dimer conformation, hydrophobic residues intervened between two APP fragments. This conformation was observed mainly in the mutant (PM1 in Figure 3b), because the mutated Leu_{29} and Leu_{33} contributed significantly. In addition to the mutated residues, Leu_{34} intervened between two APP fragments. Therefore, this form was also observed in the WT as a minor conformation. In contrast, in the third type of dimer conformation, two APP fragments crossed with each other at Gly_{38}. This conformation is similar to the conformation of glycophorin A, which also has a Gly-XXX-Gly motif in the TM region.[11] This conformation populated roughly 28.5% in the mutant (in PM2, Figure 3c),

whereas it represented less than 1.0% in the WT. The Gly-rich portion of the TM and JM regions in the WT would be too flexible to take on this conformation.

How do the conformational differences between the WT and the mutant affect the secretion of Aβ or the cleavage by γ-secretase? As shown in Figure 2, the γ-site ($Gly_{38}-Thr_{43}$) in the mutant is shifted downward by ∼3 Å along the bilayer normal. In addition, the conformational flexibility of the γ-site might be increased in the mutant because of the lack of interfragment $C_\alpha-H\cdots O$ hydrogen bonds at Gly_{38}. These changes likely induce mismatched interactions between the γ-site of APP-C99 and the active site of γ-secretase, which would reduce the secretion of $A\beta_{1-40}$ or $A\beta_{1-42}$.[5]

In summary, we have predicted the APP fragment ($A\beta_{23-55}$) dimer structures of the WT and a mutant protein using REMD simulations and found drastic changes in the dimer structures due to the mutation.[5] The results are in good agreement with the existing experimental data[5,10] and provide fundamental insight into the initial steps in the amyloid formation.

Supporting Information Available: Simulation methods, Supporting Figures 1−6, and complete ref 6b (as ref 2 in the reference list). This material is available free of charge via the Internet at http://pubs.acs.org.

References

(1) See for instance: Haass, C.; Selkoe, D. J. *Nat. Rev. Mol. Cell Biol.* **2007**, *8*, 101–112.
(2) See for instance: (a) Petkova, A. T.; Yau, W.-M.; Tycko, R. *Biochemistry* **2006**, *45*, 498–512. (b) Nelson, R.; Eisenberg, D. *Curr. Opin. Struct. Biol.* **2006**, *16*, 260–265.
(3) There are number of papers. See, for example: (a) Tarus, B.; Straub, J. E.; Thirumalai, D. *J. Am. Chem. Soc.* **2006**, *128*, 16159–16168. (b) Tarus, B.; Straub, J. E.; Thirumalai, D. *J. Mol. Biol.* **2005**, *345*, 1141–1156. (c) Massi, F.; Peng, J. W.; Lee, J. P.; Straub, J. E. *Biophys. J.* **2001**, *80*, 31–44.
(4) (a) Sugita, Y.; Okamoto, Y. *Chem. Phys. Lett.* **1999**, *314*, 141–151. (b) Miyashita, N.; Straub, J. E.; Thirumalai, D., to be published.
(5) Kienlen-Campard, P.; Tasiaux, B.; Hees, J. V.; Li, M.; Huysseune, S.; Sato, T.; Fei, J. Z.; Aimoto, S.; Courtoy, P. J.; Smith, S. O.; Constantinescu, S. N.; Octave, J. N. *J. Biol. Chem.* **2008**, *283*, 7733–7744.
(6) (a) Feig, M.; Karanicolas, J.; Brooks, C. L. *J. Mol. Graphics Modell.* **2004**, *22*, 377–395. (b) MacKerell, A. D., Jr.; et al. *J. Phys. Chem. B* **1998**, *102*, 3586–3616.
(7) Lazaridis, T. *Proteins* **2003**, *52*, 176–192.
(8) Kabsch, W.; Sander, C. *Biopolymers* **1983**, *22*, 2577–2637.
(9) (a) Kitao, A.; Go, N. *Curr. Opin. Struct. Biol.* **1999**, *9*, 164–169. (b) García, A. E. *Phys. Rev. Lett.* **1992**, *68*, 2696–2699.
(10) Sato, T.; Tang, T.; Reubins, G.; Fei, J. Z.; Fujimoto, T.; Kienlen-Campard, P.; Constantinescu, S. N.; Octave, J. N.; Aimoto, S.; Smith, S. O. *Proc. Natl. Acad. Sci. U.S.A.* **2009**, *106*, 1421–1426.
(11) (a) MacKenzie, R. A.; Prestegard, J. H.; Engelman, D. M. *Science* **1997**, *276*, 131–133. (b) Senes, A.; Ubarretxena-Belandia, I.; Engelman, D. M. *Proc. Natl. Acad. Sci. U.S.A.* **2001**, *98*, 9056–9061.

JA809227C